Computers and Chemical Engineering **(2009)**
DOI: http://dx.doi.org/10.1016/j.compchemeng.2009.07.003
Accepted postprint

Determination of optimum gas holdup conditions in a three-phase fluidized bed by genetic algorithm

H. M. Jena[a*], G. K. Roy[a] and S. S. Mahapatra[b]

[a]*Department of Chemical Engineering, National Institute of Technology (NIT), Rourkela, Orissa, Pin - 769008, India*

[b]*Department of Mechanical Engineering, National Institute of Technology (NIT), Rourkela, Orissa, Pin - 769008, India*

*Correspondence Authors Email: hara.jena@gmail.com

Abstract

Experiments have been carried out in a 0.1 m internal diameter, 1.88 m height vertical Plexiglas column with an antenna type modified air sparger in the gas-liquid distributor section. This arrangement provides uniform mixing of the fluids, ensures the gas entering the fluidizing section as fine bubbles and reduces the pressure drop encountered through a conventional distributor used for the purpose. The important dimensionless groups which have influence on the gas holdup have been developed by the use of Buckingham Pi theorem. The relation of gas holdup with these dimensionless groups has been expressed in the form of a power law equation developed with very high correlation coefficient. Residual analysis has been carried out to validate the regression model. The optimum operating conditions for maximum gas holdup in a cocurrent three-phase fluidized bed have been predicted using genetic algorithm.

Key words: Gas-liquid-solid fluidization; Multiphase flow; Gas holdup; Genetic algorithm; Optimization

1. Introduction

Three-phase fluidized beds are used in a wide range of industrial applications including processing of hydrocarbons, in particular in the upgrading of heavy oil and high molecular weight feedstock's, aerobic wastewater treatment, and direct coal liquefaction (Ramachandran and Chaudhari, 1983, Fan 1989, Nigam & Schumpe, 1996, Jena et al. 2009). The gas holdup is one of the most important characteristics for analyzing the performance of a three-phase fluidized bed. For chemical processes where mass transfer is the rate limiting step, it is important to estimate the gas holdup since this relates directly to the mass transfer (Fan et al. (1987); Schweitzer et al. (2001). Jena et al. (2008) have reviewed the considerable

work carried out on the gas holdup in three-phase fluidized beds, which focuses its dependency on various system and operating parameters. Although gas holdup in three phase fluidized beds have received significant attention as summarized in various reviews, in most of the previous work air, water, and small glass beads have been used as the gas, liquid, and solids, respectively. This combination limits the generality and usefulness of the results. The gas holdup in such systems is often considerably lower than for pilot-plant or industrial-scale units (Safoniuk et al., 2002).

Industrial-scale units operate with high gas holdup and contain small bubbles: these conditions result from effects of both high reactor pressures and low surface tension liquids. Attempts have been made by various investigators to simulate the small bubble behaviour of the ebullated bed reactor under atmospheric conditions by the use of a liquid or a liquid solution having special properties in the laboratory experimental systems (Fan et al., 1987; Safoniuk et al., 2002, Song et al., 1989). With the use of high viscous and low surface tension liquids, the gas hold up is enhanced due to the following reasons. Higher liquid viscosity exerts higher drag on the gas bubble; the same is done by lower surface tension of liquid due to formation of surface tension gradient on the bubble surface. A higher drag results in lower bubble rise velocities and hence higher holdup. With the lower surface tension of the liquid finer bubbles are formed. In using pure low surface tension liquids the initially formed finer bubbles later undergo coalescence and eventually increase in size if in the solid phase fine particles are used whose bubble breaking behaviour is not adequate. In such situations surfactants are used which promote a non-coalescing tendency in the rising gas bubbles. Similar results are obtained, where moderately high viscosity and moderately low surface tension are desirable by using aqueous solutions of glycerol as the liquid phase.

The gas holdup characteristic depends upon the bubble size and its dispersion in the bed. Thus the generation of fine gas bubbles is important which is possible by a suitable

design of the air sparger (Thorat et al., 1998). Although the use of various types of sparger is seen in the literature, but little attention has been paid to the precise design of an air sparger which can avoid the high pressure drop in the distributor section. In the present study, an antenna type air sparger has been used, as it is quite efficient in producing fine air bubbles with less pressure drop in the distributor section. Use of such an air sparger also reduces the pressure drop in the distributor section that occurs in a conventional design, and this has already been verified by Meikap et al. (2002).

The various methods of measurement of gas holdup in a gas-liquid-solid fluidized bed have been reviewed by Fan (1989) and recently by Jena et al. (2008). Larachi et al. (2001) in their work developed most generalized correlations by two different approaches using an extensive database. The first approach relies on the combination of multilayer perceptron artificial neural networks and dimensional analysis (ANN-DA). The second method is based on a phenomenological hybrid k-x generalized bubble wake model (k-x GBWM). Although the predictions of gas holdup using these can be made on a very wide range of operating conditions, but the predictions deviate largely from some specific operational conditions. No literature is found which prescribes the optimum operating conditions to maximize the gas holdup in a three-phase fluidized bed.

In the present investigation, an attempt has been made to study the gas holdup characteristics of a three-phase fluidized bed in a broader range of operation. Experiments have been conducted to examine the gas holdup of a co-current gas-liquid-solid three-phase fluidized bed with a modified air sparger using liquid as the continuous phase and gas as the discontinuous phase. Spherical glass beads have been used as the solid phase. An antenna type air sparger has been used for the generation of fine bubbles. The experimental set-up used in this work will ultimately be used as an aerobic bioreactor for the treatment of industrial waste water, where moderately high viscous and moderately low surface tension

effluent is often expected. Thus in this work the liquid phase used is tap water and aqueous glycerol solution. The experimental results have been presented graphically and their behaviour has been discussed. Empirical equations have been developed from the traditional regression analysis as well as nonlinear regression analysis using SYSTAT R7 software. Optimum operating conditions have been predicted for maximum gas holdup using Genetic Algorithm (GA).

2. Experimental

A schematic representation of the experimental setup is shown in Fig. 1. The experimental fluidized bed consists of three sections, viz., the test section, the gas-liquid distributor section, and the gas-liquid disengagement section. The test section is the main component of the fluidizer where fluidization takes place. It is a vertical cylindrical Plexiglas column of 0.1 m internal diameter and 1.88 m long. The entrained particles are retained on the 16-mesh screen attached to the top of the column. The gas-liquid distributor is located at the bottom of the test section and is designed in such a manner that uniformly distributed liquid and gas mixture enters the test section. The distributor section made of Perspex is fructo-conical of 0.31 m in height, and has a divergence angle of 4.5^0 with one end of 0.0508 m in internal diameter and the other of 0.1 m in internal diameter. The liquid inlet of 0.0254 m in internal diameter is located centrally at the lower cross-sectional end. The higher cross-sectional end is fitted to the test section, with a perforated distributor plate made of G.I. sheet of 0.001 m thick, 0.12 m diameter having open area equal to 20 % of the column cross-sectional area with a 16 mesh (BSS) stainless steel screen in between. Totally 288 numbers of 0.002, 0.0025 and 0.003 m holes have been drilled in triangular pitch made in 10 concentric circles of nearly 0.005 m radial gap. The size of the holes has been increased from inner to outer circle. This has been done with a view to have less pressure drop at the distributor plate and a uniform flow of the fluids into the test section. There is an antenna-type air sparger of

0.09 m diameter just below the distributor plate containing 50 number of 0.001 m holes, for generating uniform air bubbles of smaller size to flow throughout the cross-section of the column. In this section, the gas and the liquid streams are merged and passed through the perforated grid. The mixing section and the grid ensured that the gas and liquid are well mixed and evenly distributed into the test section. The gas-liquid disengagement section at the top of the column is a cylindrical section of 0.26 m internal diameter and 0.34 m height, assembled to the test section with 0.08 m of the test section inside it, which allows the gas to escape and liquid to be circulated through the outlet of 0.0254 m internal diameter at the bottom of this section. For pressure drop measurement in the bed, the pressure ports at each 10 cm interval have been fitted to the manometers filled with carbon tetrachloride.

The scope of the experiment is presented in Table 1. Accurately weighed amount of material was fed into the column and adjusted for a specified initial static bed height. Liquid was pumped to the fluidizer at a desired flow rate using calibrated rotameter. The air was then injected into the column through the air sparger at a desired flow rate. Approximately five minutes was allowed to make sure that the steady state was reached. The readings for pressure drop and the expanded heights of the bed were then noted. The temperature was maintained at 30 ± 2^0C. The gas holdup was determined from the pressure drop measurements using Eq. (1).

$$\varepsilon_g = \frac{(\Delta p^{ls} - \Delta p^{gls})/(\rho_L g)}{h_e} \tag{1}$$

The procedure was repeated for different liquids, particles of different sizes and at varying initial static bed heights. In this communication a few additional experiments using particle sizes 1.55 mm and 6.29 mm and liquids with varying viscosity and surface tension have been carried out and other data have been taken from a recent publication of the author

Jena et al. (2008). The main aim of this work is to develop a more precise empirical model and to optimize the operating conditions for gas holdup.

3. Results and discussion

3.1 Dimensional analysis

An industrial three-phase fluidized bed can be simulated and scaled up perfectly from a laboratory small-scale cold flow model by developing an extensive set of dimensionless groups from dimensional analysis of transport equations. The scaling is proper if the dimensionless groups are perfectly respected. Both geometric and dynamic similarity should be considered for understanding and developing correlations those can provide predictions which are valid for industrial units. In doing so the first step is to identify all variables that are expected to have a significant effect on the gas holdup dynamics. Then an appropriate set of dimensionless groups can be developed by applying Buckingham Pi theorem.

Previous studies on three-phase fluidized beds by Fan et al. (1987), Safoniuk et al (1999), and Jena et al. (2008) have identified ten variables (U_L, U_g, μ_L, σ_L, ρ_L, $\Delta\rho g$, ρ_p, d_p, h_s, D_c) which are expected to influence the gas holdup significantly. The gas density has been incorporated in the buoyancy ($\Delta\rho g$). Using these ten significant variables which involve three fundamental dimensions (mass, length and time), seven independent dimensionless groups can be formed according to Buckingham Pi theorem. Keeping in mind the advantage of using groups that are familiar in multiphase flow, two sets of seven independent dimensionless groups has been developed by rearrangement as;

Set-1: $\mathrm{Re}_L = \dfrac{\rho_L D_c U_L}{\mu_L}$, $Fr_g = \dfrac{U_g^2}{gD_c}$, $We = \dfrac{\rho_L D_c U_L^2}{\sigma_L}$, $\Delta\beta_d = \dfrac{(\rho_L - \rho_g)}{\rho_L}$, $\beta_d = \dfrac{\rho_p}{\rho_L}$,

$d_r = \dfrac{d_p}{D_c}$, and $h_r = \dfrac{h_s}{D_c}$

Set-2: $Mo = \frac{g\mu_L^4}{\rho_L \sigma_L^3}$, $Eo = \frac{\Delta\rho g D_c^2}{\sigma_L}$, $Fr_L = \frac{U_L^2}{gD_c}$, $Fr_g = \frac{U_g^2}{gD_c}$, $\beta_d = \frac{\rho_p}{\rho_L}$, $d_r = \frac{d_p}{D_c}$, and $h_r = \frac{h_s}{D_c}$

The combinations Weber number (*We*), Reynolds number (*Re*), and Froude number (*Fr*) or Morton number (*Mo*) and Eötvös number (*Eo*) are used to characterize the multiphase flow of bubbles or drops moving in a surrounding fluid. Morton number (*Mo*) is the combination of Weber number (*We*), Reynolds number (*Re*), and Froude number (*Fr*). Previous work by Fan et al. (1987) and Safoniuk et al. (1999) have stressed on Morton number (*Mo*) and Eötvös number (*Eo*) than Weber number (*We*). In the present work it has also been found that the second set gives better value of coefficient of determination (R-square) in developing the model equation. Therefore in the present study we have used the second set for analysis of the gas holdup dynamics.

3.2 Gas holdup dynamics

Fig. 2 shows the variation of fractional gas holdup with liquid Froude number at different values of fixed gas Froude number. It is seen from the figure that with increasing liquid Froude number, the gas holdup decreases. However the variation of fractional gas holdup with liquid Froude number is small. At higher liquid Froude number large number of fine bubbles are possible as the flow regime is completely distributed or dispersed, for which the gas holdup should be more. But the decrease in gas holdup with liquid Froude number may possibly be due to the fact that at higher liquid Froude number the bubbles are fast driven by the liquid. The residence time of the bubbles decreases with the liquid Froude number and hence the gas holdup is likely to decrease.

Fig. 3 represents the variation of fractional gas holdup with gas Froude number, at constant liquid Froude numbers. As seen from the figure, the fractional gas holdup increases

monotonically with the gas Froude number having higher value of the slope at low gas Froude numbers. In the lower range of gas Froude number, an increase in gas Froude number results in the formation of a larger number of gas bubbles without appreciable increase in the bubble diameter. Therefore an increasing fractional gas holdup is observed. As gas velocity increases, the bubble size grows due to bubble coalescence, and relatively the slope of gas holdup line decreases. The decrease in slope may be due to the transformation of flow from bubble to the slug flow regime.

In Fig. 4 the variation of fractional gas holdup with liquid Froude number has been represented for different ratios of particle size to column diameter keeping all other variables constant. As the density of particles of different size is different there is a variation of the ratio of density of particle to the density of the liquid as mentioned in the figure. The gas holdup decreases with liquid velocity like the above finding. But the measured gas holdup is found to increase with particle size. A significant variation of the fractional gas holdup is seen between the particle sizes of 2.18 and 4.05mm, but the variation magnitude is less for particles smaller than 2.18 mm and larger than 4.05mm. Higher gas holdup for bigger size particles may be attributed to their enhanced bubble breaking capacity. Kim et al. (1975) used glass beads of 1 mm and 6 mm in their study and have reported the existence of two distinct types of three-phase fluidized beds, viz., “bubble coalescing” and “bubble disintegrating” beds. According to them 6 mm glass beads in air-water system exhibited bubble disintegrating behaviour. However 1 mm glass beads exhibited bubble coalescing behaviour. They have reported the existence of critical particle size which separates the “bubble coalescing regime” from the “bubble disintegrating regime”. The critical size for particles with a density similar to that of glass has been reported by them to be about 2.5 mm in diameter for the air-water system. This seems to be a well fit to the present experimental finding. The difference in gas holdup for particles of different size is more in the higher

liquid Froude number. This may be due to the better fluid particle interaction and higher mass of particles adds up to its bubble breaking behaviour in such a situation, thus resulting in large number of small size bubbles. The investigation of Dargar and Macchi (2006) also indicates the same behaviour for air-water system. They have used 1.2 mm and 5 mm glass beads. Higher gas holdup has been reported by them for 5 mm size glass beads over the other sizes. Fan et al. (1987) have shown opposite behaviour for 1, 3, 4, and 6 mm glass beads in aqueous solution of 0.5-wt% of t-pentanol. With increase in particle size, reduced gas holdup has been reported by them.

The variation of fractional gas holdup with liquid Froude number for different ratios of the initial static bed height (static bed inventories) to the column diameter (h_s/D_c) at constant values of other variables are shown in Fig. 5. It is clear from the figure that at low liquid Froude number range the gas holdup is almost same for different values of h_s/D_c. But at high liquid Froude number range, i.e. at higher bed voidage, there is a little increase in the gas holdup with h_s/D_c. This may possibly be due to the gas-liquid-solid interaction for a longer time in the bed for higher initial static bed height or h_s/D_c. Study on the effect of bed inventory on gas holdup is not seen in the literature.

Fig. 6 represents the variation of fractional gas holdup with gas Froude number for different liquid solutions, at constant values of liquid Froude number, d_p/D_c, h_s/D_c. Similar trend of gas holdup with the variation of gas Froude number has been observed in this case as it was represented in Fig. 3. As represented in Fig. 6, due to variation of the liquid density, viscosity and surface tension with aqueous solutions of glycerol, there is a change in Morton number (*Mo*) and Eötvös number (*Eo*) and ρ_p/ρ_L. With increase in both Morton number (*Mo*) and Eötvös number (*Eo*), the gas holdup is found to increase. Similar results have been obtained by other investigators like Fan et al. (1987), Song et al. (1989), Safoniuk et al. (1999 and 2002). The enhancement of gas hold up with the use of high viscous and low surface

tension liquids is due to the following reasons. Higher liquid viscosity exerts higher drag on the gas bubble; the same is done by lower surface tension of liquid due to formation of surface tension gradient on the bubble surface. A higher drag results in lower bubble rise velocities and hence higher holdup. Lower surface tension of liquids also makes the generation and existence of fine bubbles possible thus by possessing higher residence time in the system increases the gas holdup.

3.3 Development of model equation

Empirical model equation has been developed to express the gas holdup behaviour from the experimental data by traditional regression analysis and least square estimation using Gauss-Newton method with the aid of SYSTAT R7 software. In the traditional regression analysis, first the dependency of the response on each individual group has been expressed as the power law relationship keeping all other groups constant as, ε_g = A1 $(Mo)^{a1}$, with *Eo*, Fr_L… etc constant, ε_g = A2 $(Eo)^{a2}$, with, *Mo*, Fr_L… etc constant. Then the response ε_g expressed as $\varepsilon_g = C((Mo)^{a1}(Eo)^{a2}(Fr_L)^{a3}\ldots)^{B}$, where A1, A2, …, C are the coefficients and a1, a2, …., B are the exponents. The following Eq. (2) has been obtained. In developing the model 36 numbers of data sets have been used. The R-square value of the developed equation is 0.972. The equation fits another 204 number of data sets with a standard deviation of 0.0695.

$$\varepsilon_g = 8\times10^{-7}(Mo)^{0.0508}(Eo)^{2.046}(Fr_L)^{-0.0789}(Fr_g)^{0.3597}(\beta_d d_r)^{0.06329}(h_r)^{0.0738} \qquad (2)$$

An attempt has been made to develop a more precise model taking large number of data sets with high R-square value and low standard deviation using non-linear regression method. Any regression analysis needs that data to be uncorrelated. Therefore, Pearson's correlation coefficient for all pairs of variables considered in this study has been calculated. The correlation analysis suggests that most of the input variables are not correlated to each

other except for a few combinations like Mo and Eo, Mo and β_d and Eo and β_d due to involvement of a common parameter like liquid density in these combinations. The correlation coefficients between the input variables and the output variable (gas holdup) are quite good and satisfy the statistical acceptable limit. Hence, the data can be reasonably assumed to be independent. Non-linear regression equation is developed based on least square estimation using Gauss-Newton method. The model so developed using software SYSTAT R7 is given as Eq. (3).

$$\varepsilon_g = (Mo)^{0.05}(Eo)^{0.157}(Fr_L)^{-0.093}(Fr_g)^{0.401}(\beta_d)^{-0.096}(d_r)^{0.081}(h_r)^{0.026} \quad (3)$$

In order to validate the model, coefficient of determination (R^2) is calculated and it is found to be 0.997. Further, residual analysis is made to check the robustness of the model. It is found that residual is normally distributed with mean 0.001 (almost zero) and standard deviation of 0.003 (very small). The frequency plot shown in Fig. 7 depicts normal distribution of the residuals. The variation of residuals with predicted values is shown in Fig. 8. It is observed that there is small fluctuation of residuals between -0.009 to 0.007 about zero. Hence, it is said that the model can predict the values with sufficient accuracy. Upper and lower confidence interval of model parameters at 95% is estimated as shown in Table 2. The experimentally found gas holdup has been compared with the ones calculated from Eqs. (2) and (3) in Fig. 9. It is seen that the Eq. (3) is a better fit to the experimental gas holdup. Thus the empirical model (Eq. (3)) is precise enough for the prediction of gas holdup and has been used to optimize the operating conditions for finding highest possible gas holdup in the experimental domain.

To check the validity of the proposed Eq. (3), experiments have been conducted at another concentration of glycerol (44% by mass of glycerol) as appeared in literature (Safoniuk et al., 2002). The experimental result has been compared with the predicted ones from Eq. (3), the correlation proposed by Safoniuk et al. (2002) for 44% glycerol solution,

the correlation of Ramesh and Murugesan (2002) and the correlations of gas holdup proposed using various surfactants (Fan et al., 1987; Gorowara and Fan, 1990) and presented in Fig. 10. It can be seen from Fig. 10 that there is a close agreement between the experimental values and those predicted from Eq. (3). The correlation of Safoniuk et al. (2002) predict higher values of gas holdup at lower gas velocities (lower Fr_g) and lower values of gas holdup at higher gas velocities, but the agreement is within 25% with the experimental values. This difference may be due to the non-existence of all other parameters except the modified gas Reynolds number in correlation of Safoniuk et al. (2002). The predicted values of gas holdup from the correlation of Ramesh and Murugesan (2002) although shows the same trend in the variation of gas holdup with Fr_g, but the predicted values are lower than the experimental ones. This is because of the air sparger used by them is a single nozzle type which might be producing large size bubbles moving centrally in the column without proper distribution. Surfactant is not a consideration in this study but as the glycerol possesses low surface tension, using glycerol the surface tension of the solution varies and its effect on the gas holdup has been expressed in the form of *Mo* and *Eo* in the proposed correlation. Fig. 10 shows that under similar flow conditions the gas holdup predicted from the correlations (Fan et al., 1987; Gorowara and Fan, 1990) developed using surfactants predict higher values of gas holdup. Above all the trend in the variation of gas holdup (both experimental and predicted from Eq. (3)) agrees well with the predicted values from correlations proposed by other investigators and the values are in agreement with those reported with the same glycerol concentration (Safoniuk et al., 2002).

3.4 Optimization of operating conditions

Hydrodynamic bahaviour of a three-phase fluidized bed is quite complex and the empirical equations used to explain the system behavior is highly nonlinear; thus making the

analysis difficult. If attempt is made to optimize process parameters (operating conditions) for maximum gas hold up, it becomes still cumbersome. As many interacting variables operate in non-linear fashion, it is difficult to obtain global solution using traditional optimization tools. Hence, parametric optimization has been done using genetic algorithm, a popular evolutionary technique, with the aim to obtain global best values with reasonable computational time and less mathematical rigor (Holland,1975).

The optimization problem for maximization gas holdup can be defined as follows:

Maximize ε_g (4)

Subjected to constraints (operating limits of each dimensionless group in the experimental domain):

$1.1078\text{x}10^{-11} \leq Mo \leq 3.3397\text{x}10^{-10}$ (5)

$1370.663 \leq Eo \leq 1527.798$ (6)

$4.59\text{x}10^{-4} \leq Fr_L \leq 2.52\text{x}10^{-2}$ (7)

$4.58\text{x}10^{-4} \leq Fr_g \leq 2.52\text{x}10^{-2}$ (8)

$2.124 \leq \beta_d \leq 2.481$ (9)

$0.0155 \leq d_r \leq 0.0629$ (10)

$1.71 \leq h_r \leq 3.01$ (11)

Genetic algorithm mainly depends on the following types of operators: reproduction, crossover, and mutation. The computational algorithm was implemented in C^{++} code. In this work, roulette wheel selection, single point crossover, and standard bit-wise mutation have been adopted. In genetic optimization, population size, probability of crossover and mutation are set at 20, 25%, and 5% respectively. Number of generation is varied till the output is converged. The flow chart of the method is depicted in Fig. 11. The optimum conditions of the group variables with the optimum performance output i.e. the maximum gas holdup are given by [Mo, Eo, Fr_L, Fr_g, β_d, d_r, h_r, ε_g] = [$3.21\text{x}10^{-10}$, 1487.57, $1.10\text{x}10^{-3}$, $1.55\text{x}10^{-2}$, 2.2797,

0.0588, 2.747, 0.282]. The convergence curve is shown in Fig. 12. The optimum gas holdup in the experimental domain is found to be 0.282. As discussed in the preceding gas holdup dynamics section 3.2, the gas holdup increases with *Mo*, *Eo*, Fr_g, d_r and h_r but decreases with Fr_L and β_d. Thus a higher gas holdup is expected at higher values of *Mo*, *Eo*, Fr_g, d_r and h_r and lower value of Fr_L and β_d. The determined maximum gas holdup in the experimental domain is not at the extreme values of these variables because of the presence interaction among the variables. The trade-off among them yields an optimum combination of the engineering groups with a maximum possible gas holdup value.

4. Conclusions

Gas holdups were measured under various operating conditions dynamically similar to some industrial reactor (fluidized bed aerobic bioreactor). By matching the geometric and dynamic similitude an industrial reactor can be scaled up with high gas holdup. The overall gas holdup has been strong function of Eötvös number and gas Froude number. Measurement of gas holdup has confirmed the known fact that the structure of the bed is different for small and large particles. The proposed empirical model (Eq. (3)) for prediction of gas holdup is found satisfactory with high value of coefficient of determination (0.997). The residual analysis shows the robustness of the model. Using Eq. (3) the operating conditions have been optimized for highest gas holdup in the experimental domain. As the empirical model represents the gas holdup dynamics to be highly nonlinear, the parametric optimization has been done using genetic algorithm. The optimum operating conditions in terms of various dimensionless groups have been found to be [*Mo*, *Eo*, Fr_L, Fr_g, β_d, d_r, h_r] = [$3.21\text{x}10^{-10}$, 1487.57, $1.10\text{x}10^{-3}$, $1.55\text{x}10^{-2}$, 2.2797, 0.0588, 2.747] with a maximum gas holdup value of 0.282 for the present system studied.

Nomenclature

A cross-sectional area of the column, m^2

D_c diameter of the column, m

d_p particle diameter, m

d_r particle diameter to column diameter ratio, (= d_p/D_c)

Eo Eötvös number, (= $\Delta\rho g D_c^2/\sigma_L$)

Fr_g gas Froude number, (= $U_g^2/(g\ Dc)$)

Fr_L liquid Froude number, (= $U_L^2/(g\ Dc)$)

g acceleration due to the gravity, ms^{-2}

h_e height of expanded bed, m

h_r bed aspect ratio, (= h_s/D_c)

h_s initial static bed height, m

Mo Morton number, (=g $\mu_L^4/(\rho_L\ \sigma_L^3)$)

Δp^{ls} pressure drop for liquid-solid fluidization, Pa

Δp^{gls} pressure drop for gas-liquid-solid fluidization, Pa

Re_L liquid Reynolds number, (= $\rho_L\ D_c\ U_L\ /\mu_L$)

Re_g modified gas Reynolds number, (= $\rho_L\ d_p\ U_g\ /\mu_L$)

U_g gas velocity, m s^{-1}

U_L liquid velocity, m s^{-1}

We Weber number, ((= $\rho_L\ D_c\ U_L^2\ /\ \sigma_L$)

Greek Symbols

β_d ratio of densities, (= ρ_p/ρ_L)

$\Delta\beta_d$ ratio of buoyancy to liquid density, (=$(\rho_L-\rho_g)/\rho_L$)

$\Delta\rho$ buoyancy term ($=\rho_L - \rho_g$), kg m^{-3}

μ_L liquid viscosity, Pa s

σ_L surface tension of liquid. kg m^{-2}

ε_g fractional gas holdup

ρ_g, ρ_L, ρ_p gas, liquid and particle density, kg m^{-3}

References

Dargar, P., and Macchi, A. (2006). Effect of Surface-Active Agents on the Phase Holdups of Three-Phase Fluidized Beds. *Chemical Engineering and Processing*, 45, 764–772.

Fan, L.S. (1989). Gas-Liquid-Solid Fluidization Engineering. Butterworth Series in Chemical Engineering, Butterworth Publishers, Boston, MA.

Fan, L.S., Bavarian, F., Gorowara, R.L., and Kreischer, B.E. (1987). Hydrodynamics of Gas-Liquid-Solid Fluidization under High Gas Hold-Up Conditions. *Powder Technology*, 53, 285-293.

Gorowara, R.L., and Fan, L.S. (1990). Effect of surfactants on three-phase fluidized bed hydrodynamics. *Industrial Engineering Chemistry and Research*, 29, 882-891.

Jena, H.M., Roy, G.K., and Meikap, B.C. (2008). Prediction of gas holdup in three-phase fluidized bed from bed pressure drop measurement. *Chemical Engineering Research and Design*, 86, 1301-1308.

Jena, H.M., Roy, G.K., and Meikap, B.C. (2009). Hydrodynamics of a gas-liquid-solid fluidized bed with hollow cylindrical particles. *Chemical Engineering and Processing: Process Intensification*, 48, 279-287.

Kim, S.P., Baker, C.G.J., and Bergougnou, M.A. (1975). Phase Holdup Characteristics of Three Phase Fluidized Beds. *Canadian Journal of Chemical Engineering*, 53, 134-139.

Larachi, F., Belfares, L., Iliuta, I., and Grandjean, B.P.A. (2001). Three-phase Fluiddization Macroscopic Hydrodynamics Revisited. *Industrial Engineering Chemistry and Research*, 40, 993-1008.

Meikap, B.C., Kundu, G., and Biswas M.N. (2002). Prediction of dispersed phase holdup in a modified multi-stage bubble column scrubber. *Canadian Journal of Chemical Engineering*, 80, 306-312.

Nigam, K. D. P., and Schumpe, A. (Eds.), (1996). Three-phase sparged reactors. Gordon and Breach: Canada, pp. 3-10.

Ramachandran, P. A., and Chaudhari, R. V. (1983). Three-phase catalytic reactors. New York: Gordon and Breach.

Ramesh, K., and Murugesan, T. (2002). Minimum fluidization velocity and gas holdup in gas-liquid-solid fluidized bed reactors. *Journal of Chemical Technology and Biotechnology*, 77, 129-136.

Safoniuk, M., Grace, J.R., Hackman, L., and Mcknight, C.A. (1999). Use of dimensional similitude for scale-up of hydrodynamics in three-phase fluidized beds. *Chemical Engineering Science*, 54, 4961-4966.

Safoniuk, M., Grace, J.R., Hackman, L., and Mcknight, C.A. (2002). Gas Hold-Up in a Three-Phase Fluidized Bed. *AIChE Journal*, 48, 1581-1587.

Schweitzer, J.M., Bayle, J., and Gauthier, T. (2001). Local Gas Hold-Up Measurements in Fluidized Bed and Slurry Bubble Column. *Chemical Engineering Science*, 56, 1103–1110.

Song, G.H., Bavarian, F., Fan, L.S. (1989). Hydrodynamics of three-phase fluidized bed containing cylindrical hydrotreating catalysts. *Canadian Journal of Chemical Engineering*, 67, 265-275.

Thorat, B.N., Shevade, A.V., Bhilegaonkar, K.N., Aglawe, R.H., Parasu Veera, U., Thakre, S.S., Pandit, A.B., Sawant, S.B., Joshi, J.B. (1998). Effect of sparger design and height to diameter ratio on fractional gas hold-up in bubble columns. *Trans IChemE Part A*, 76, 823-834.

Holland J.H. (1975). Adaptation in natural and artificial systems. MIT Press, Cambridge, MA.

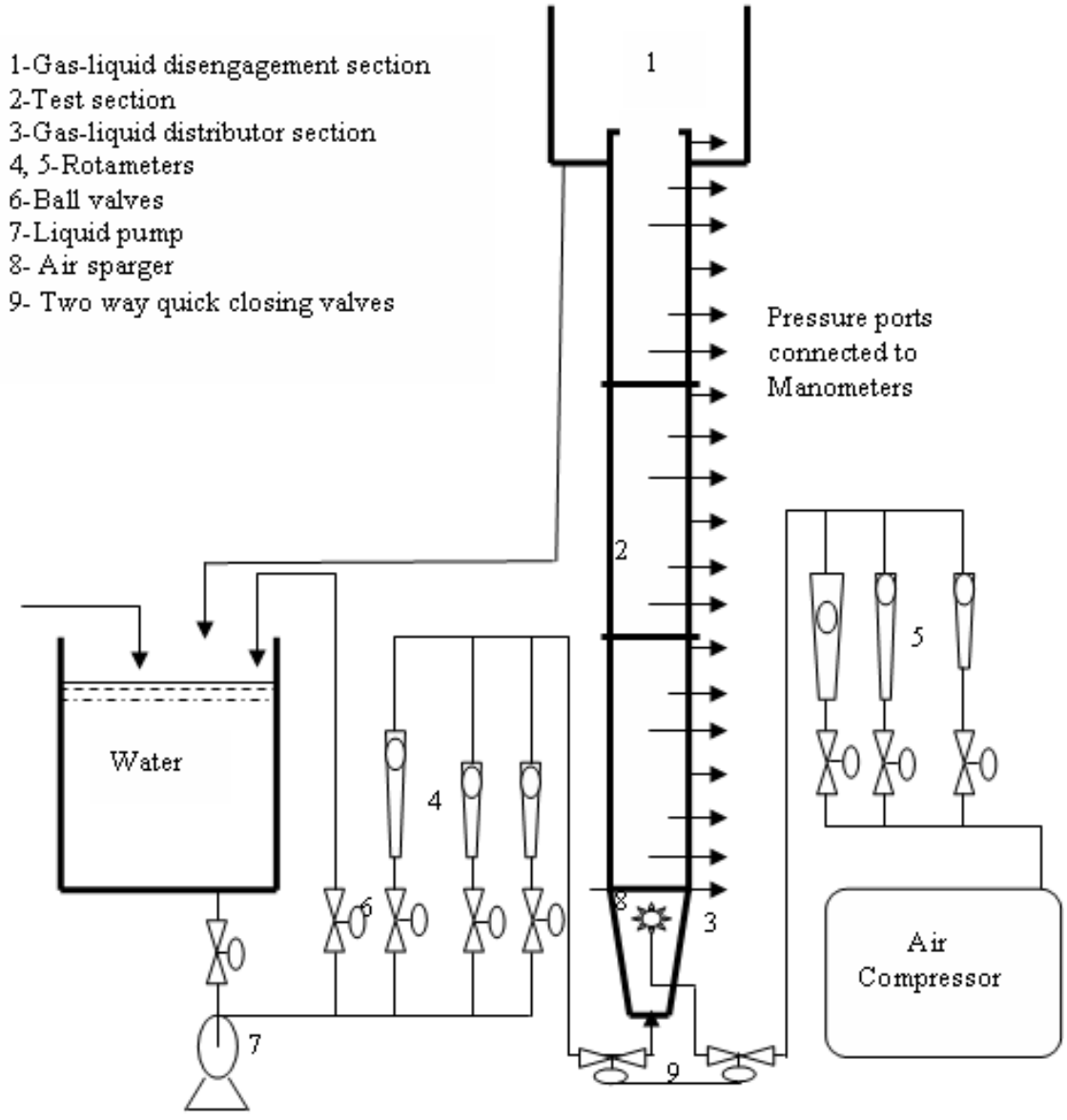

Fig. 1. Schematic representation of the three-phase fluidized bed.

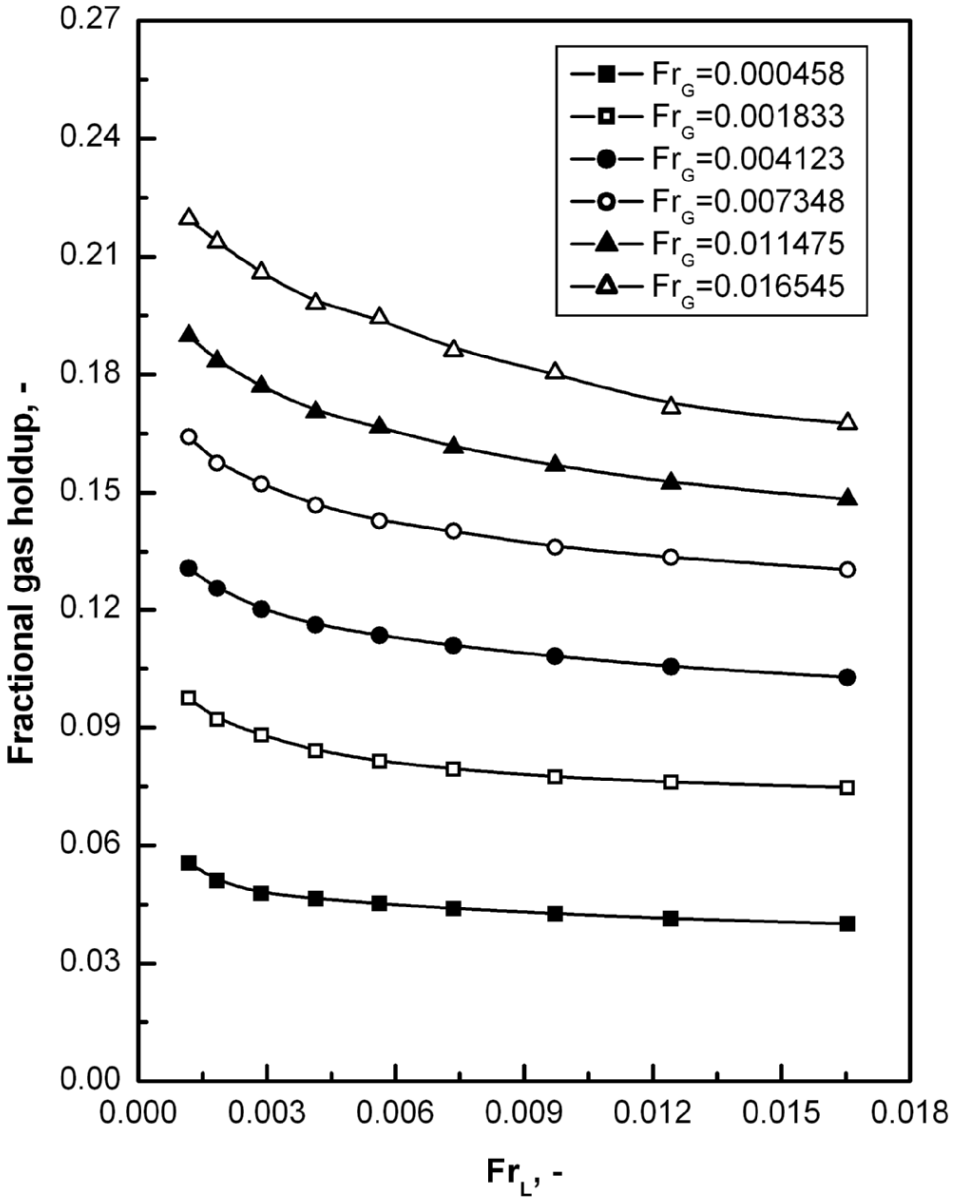

Fig. 2. Variation of gas holdup with liquid Froude number for different gas Froude number at [h_s/D_c = 2.56, d_p/D_c = 0.0307, ρ_P/ρ_L = 2.263, M = 1.1078×10^{-11} and Eo = 1370.66].

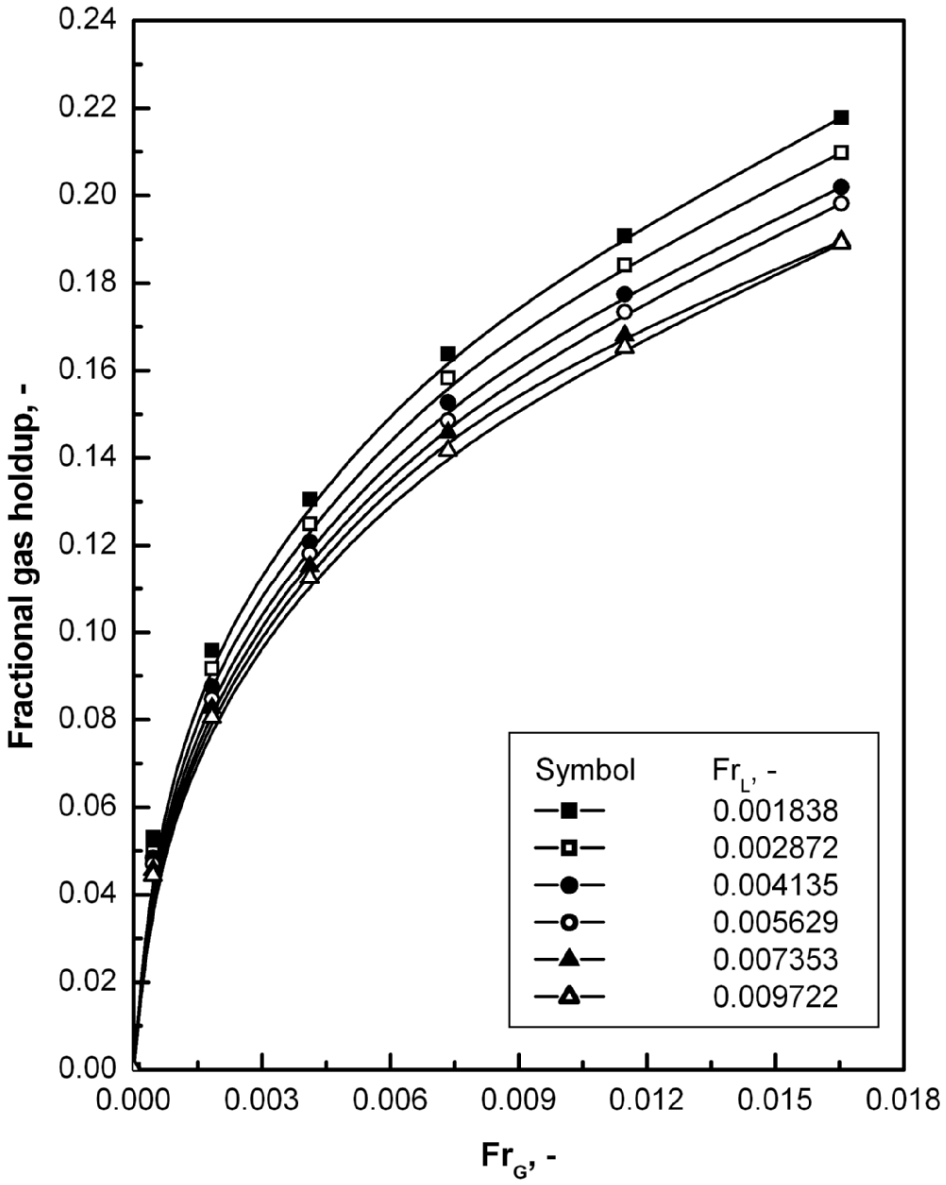

Fig. 3. Variation of gas holdup with gas Froude number for different liquid Froude number at [h_s/D_c = 2.56, d_p/D_c = 0.0405, ρ_P/ρ_L = 2.270, M = 1.1078x10^{-11} and Eo = 1370.66].

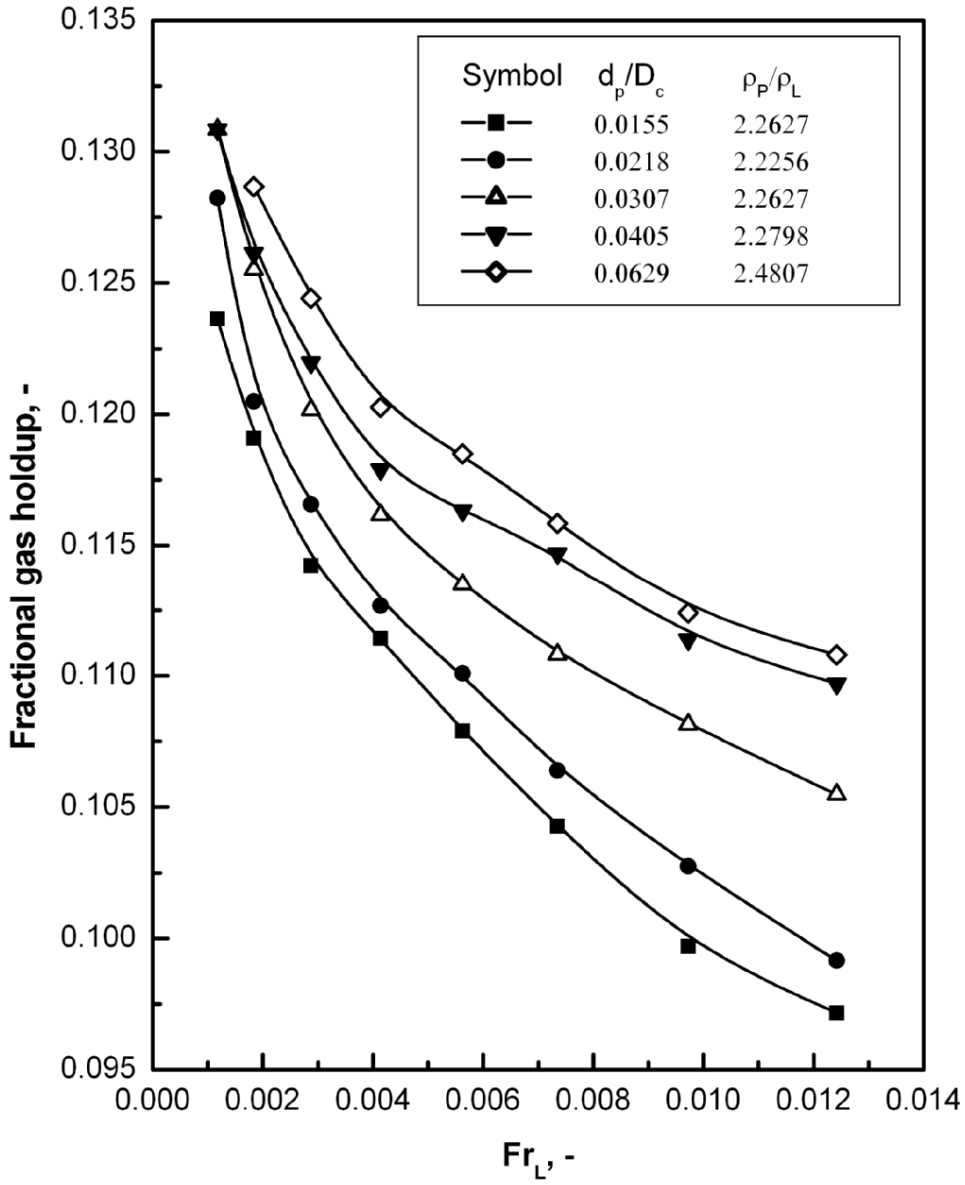

Fig. 4. Variation of gas holdup with liquid Froude number for different d_p/D_c at [h_s/D_c = 2.56, Fr_G = 0.004123, M = 1.1078×10^{-11} and Eo = 1370.66].

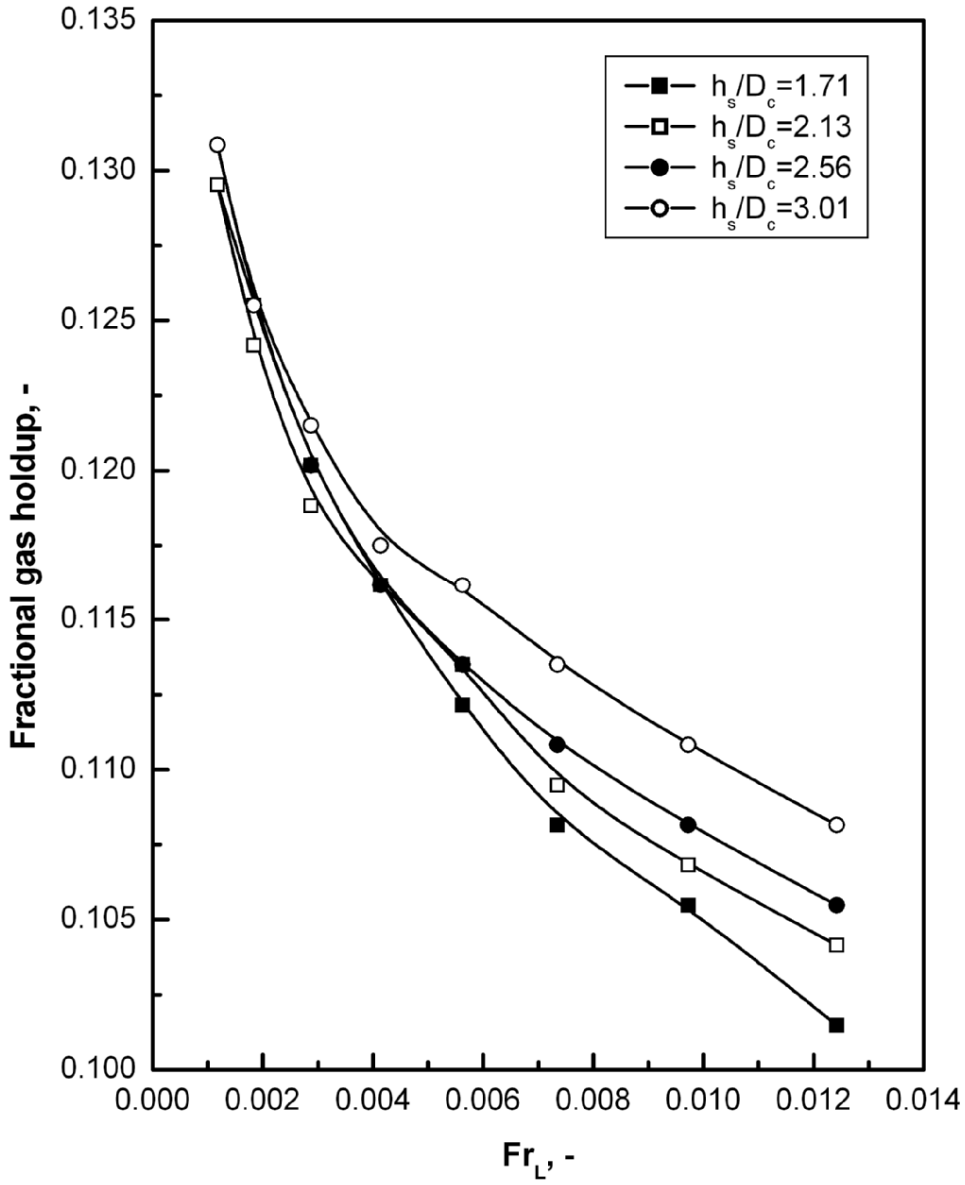

Fig. 5. Variation of gas holdup with liquid Froude number for different h_s/D_c at [d_p/D_c = 0.0307, ρ_P/ρ_L = 2.263, Fr_G = 0.004135, M = 1.1078x10^{-11} and Eo = 1370.66].

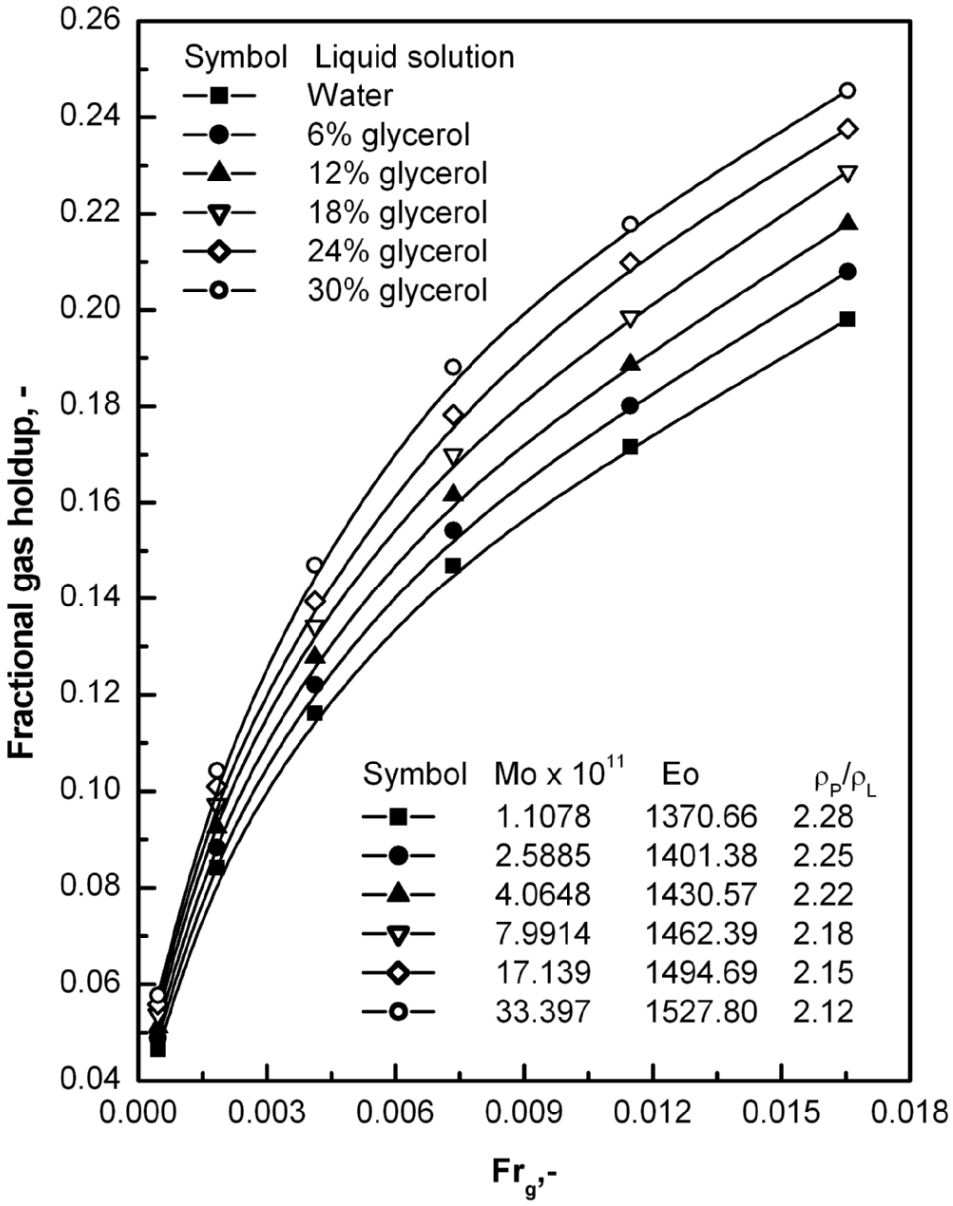

Fig. 6. Variation of gas holdup with gas Froude number for different liquids at [h_s/D_c = 2.56, d_p/D_c = 0.0405, Fr_L = 0.004135].

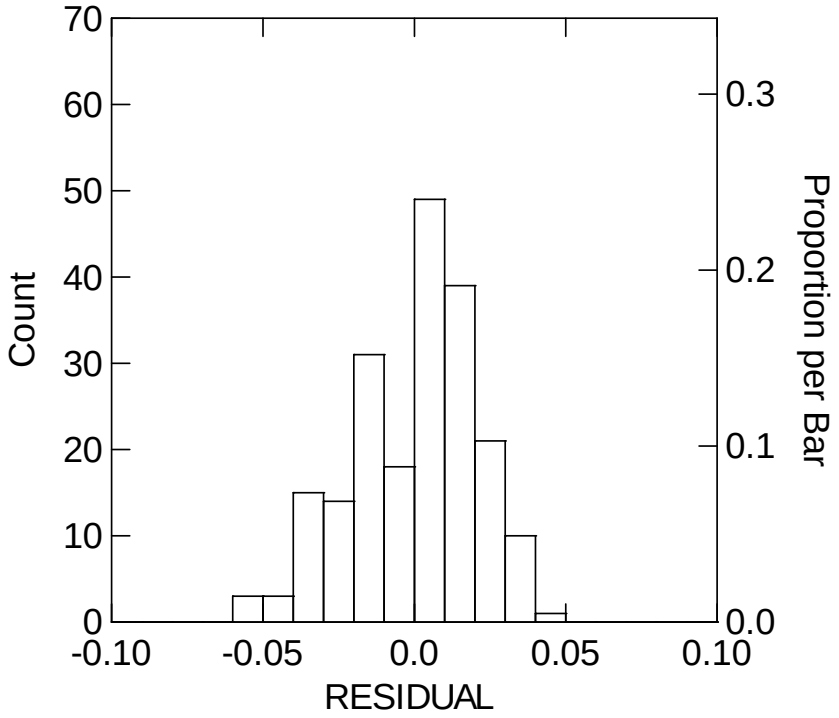

Fig. 7. Frequency plot of residuals

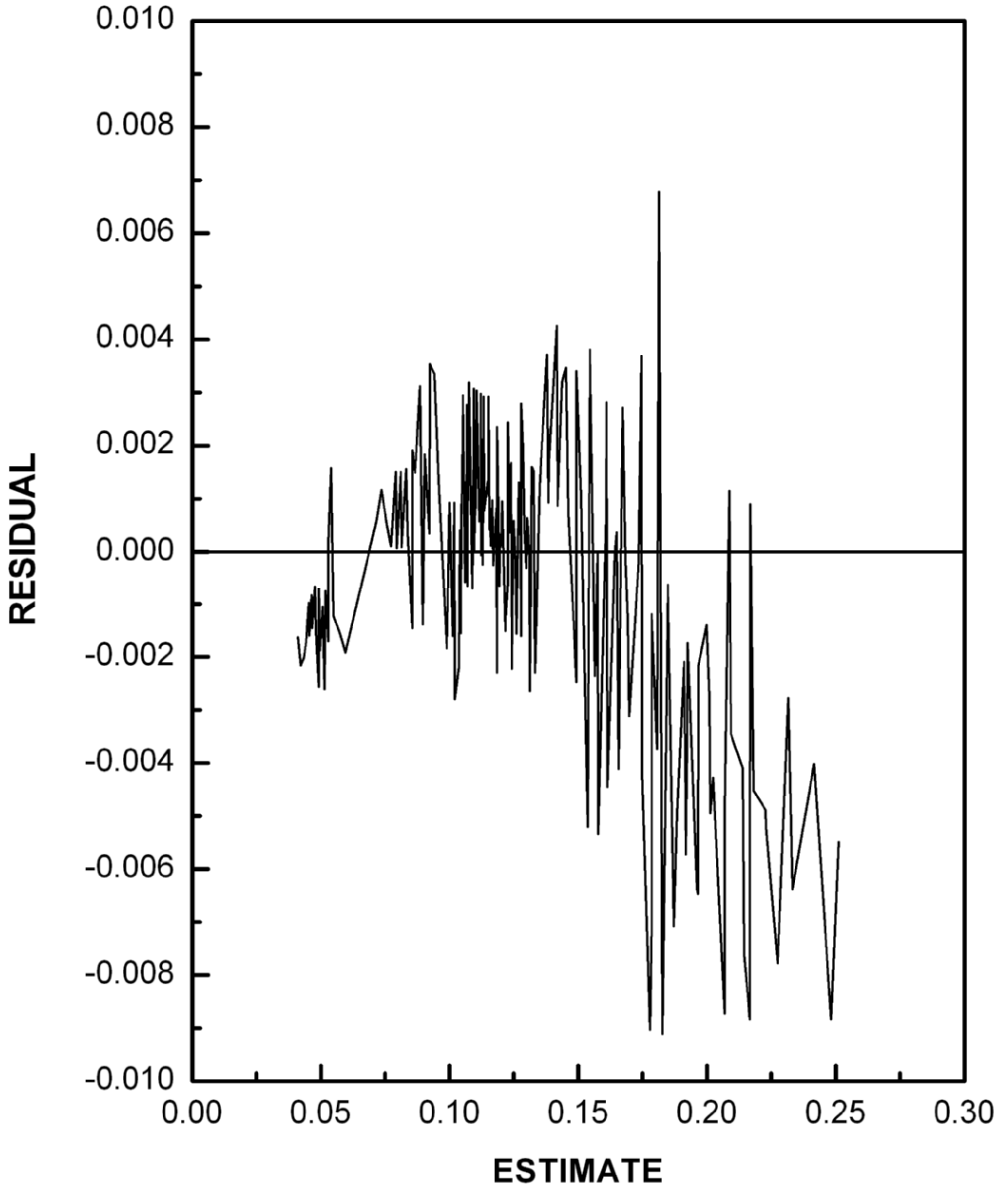

Fig. 8. Distribution of residuals.

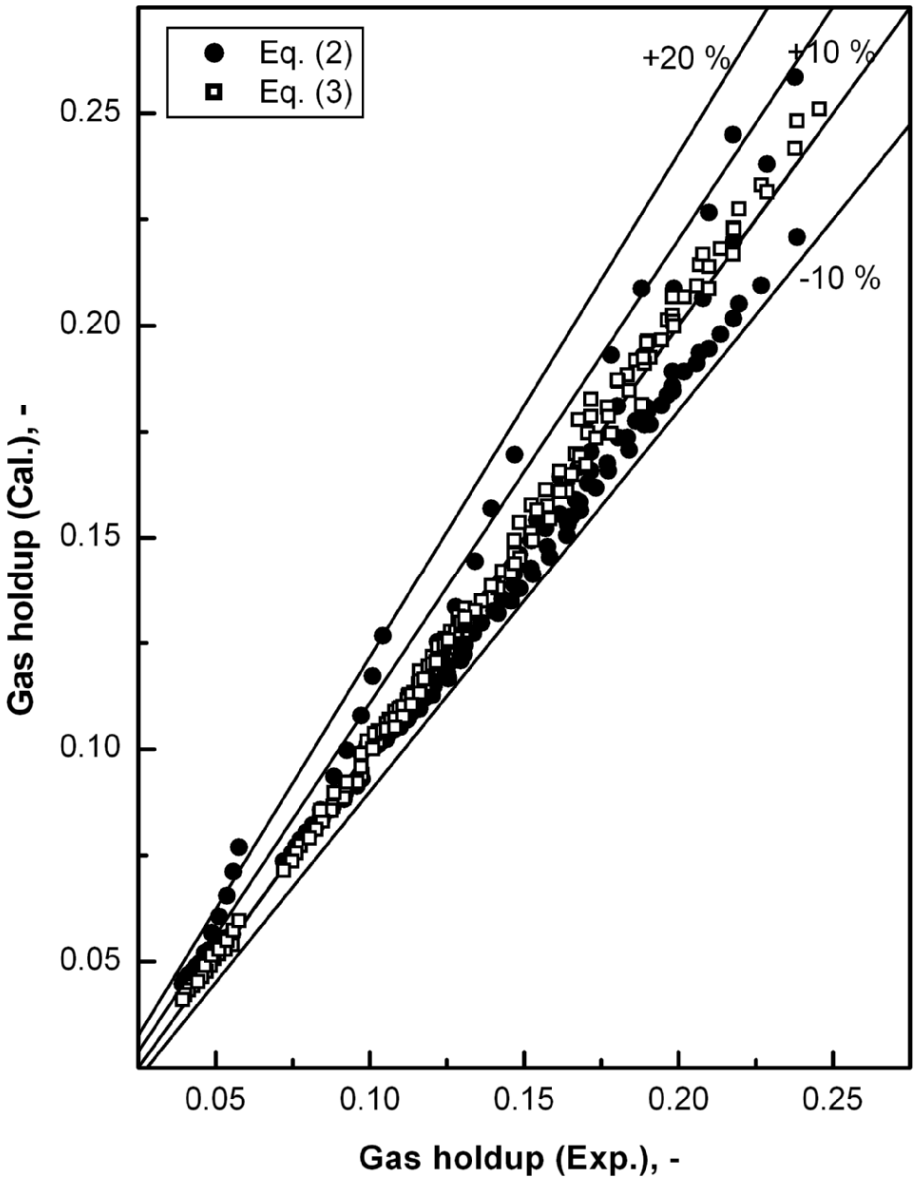

Fig. 9. Comparison of gas holdup.

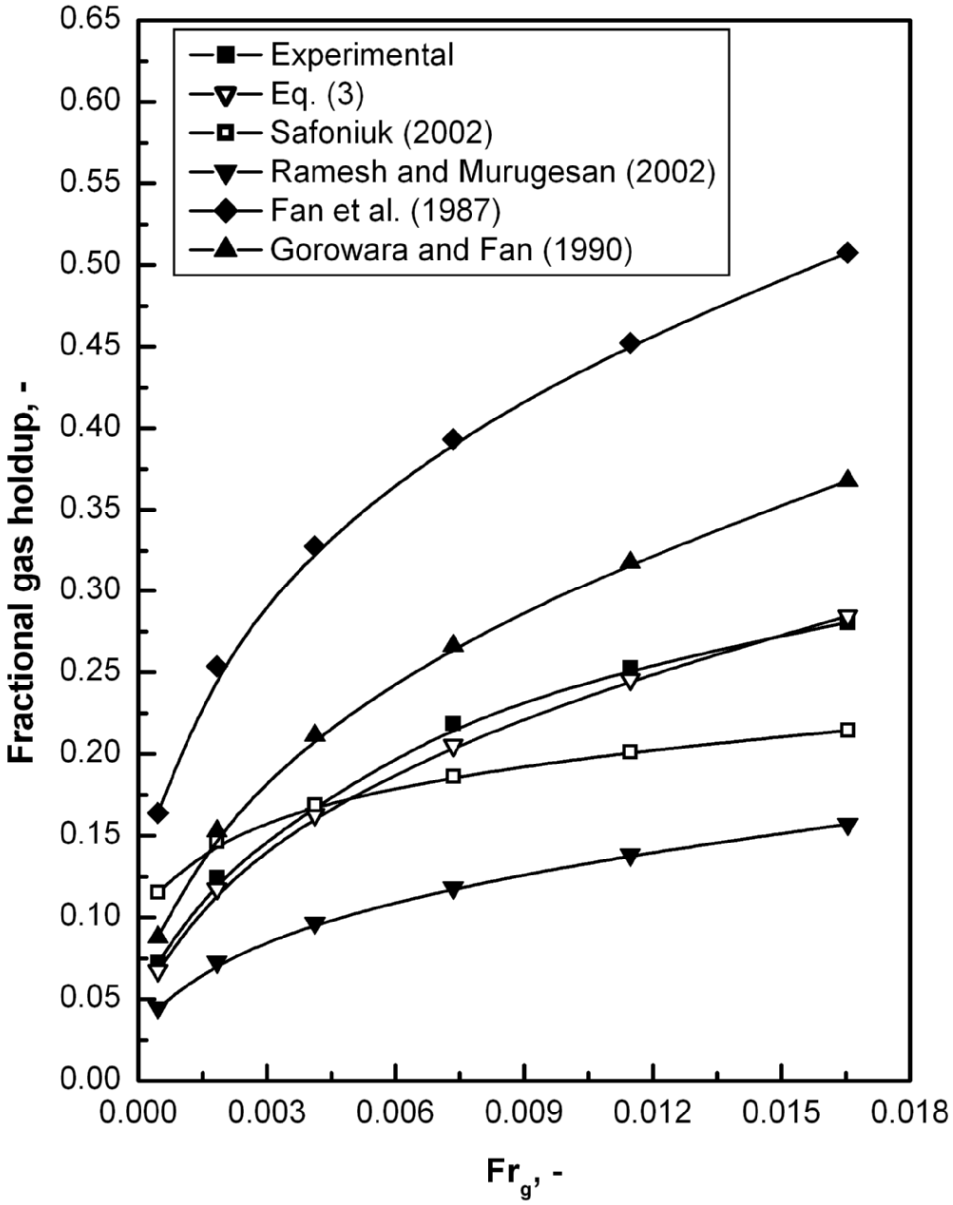

Fig. 10. Comparison with literature correlations.

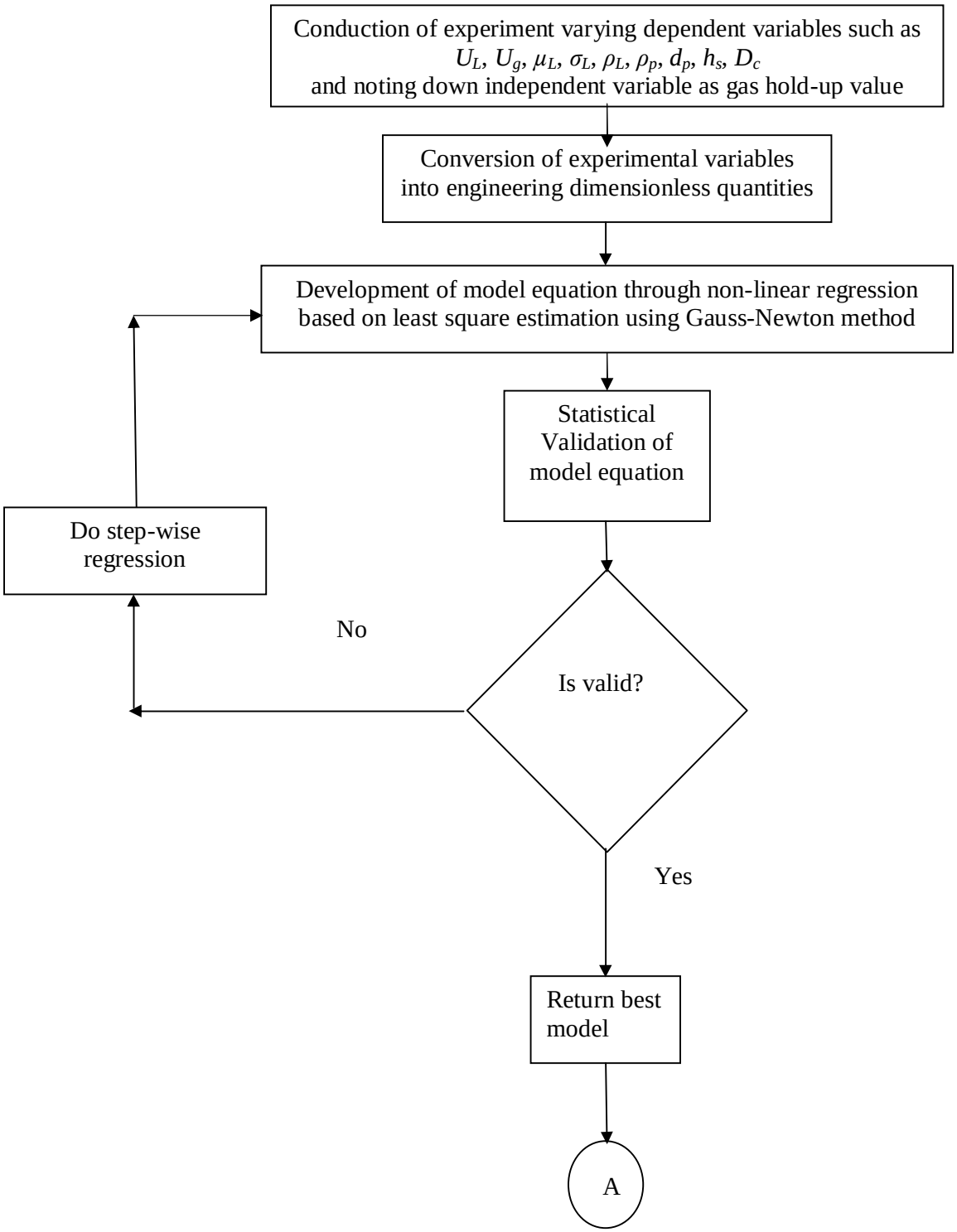

Fig. 11. Flow chart of the method.

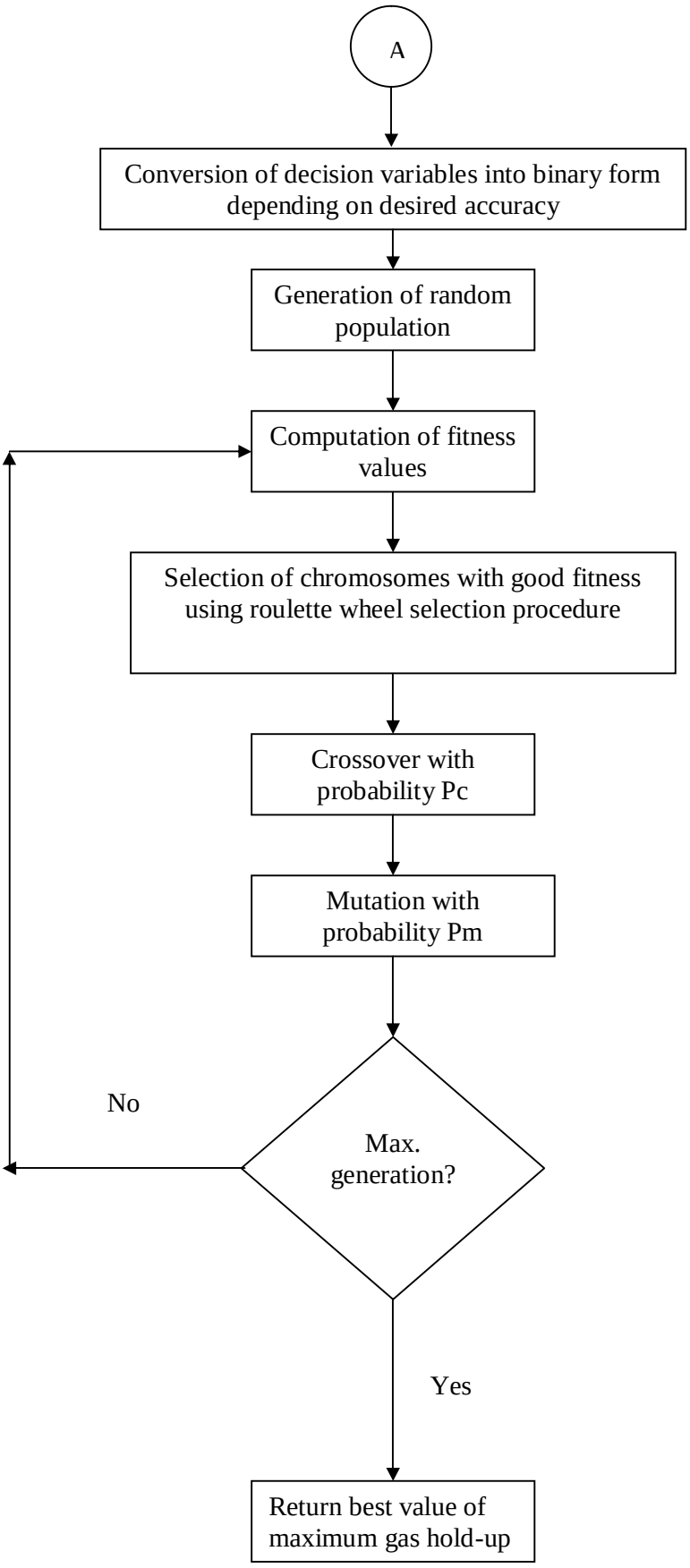

Fig. 11. (*Continued*).

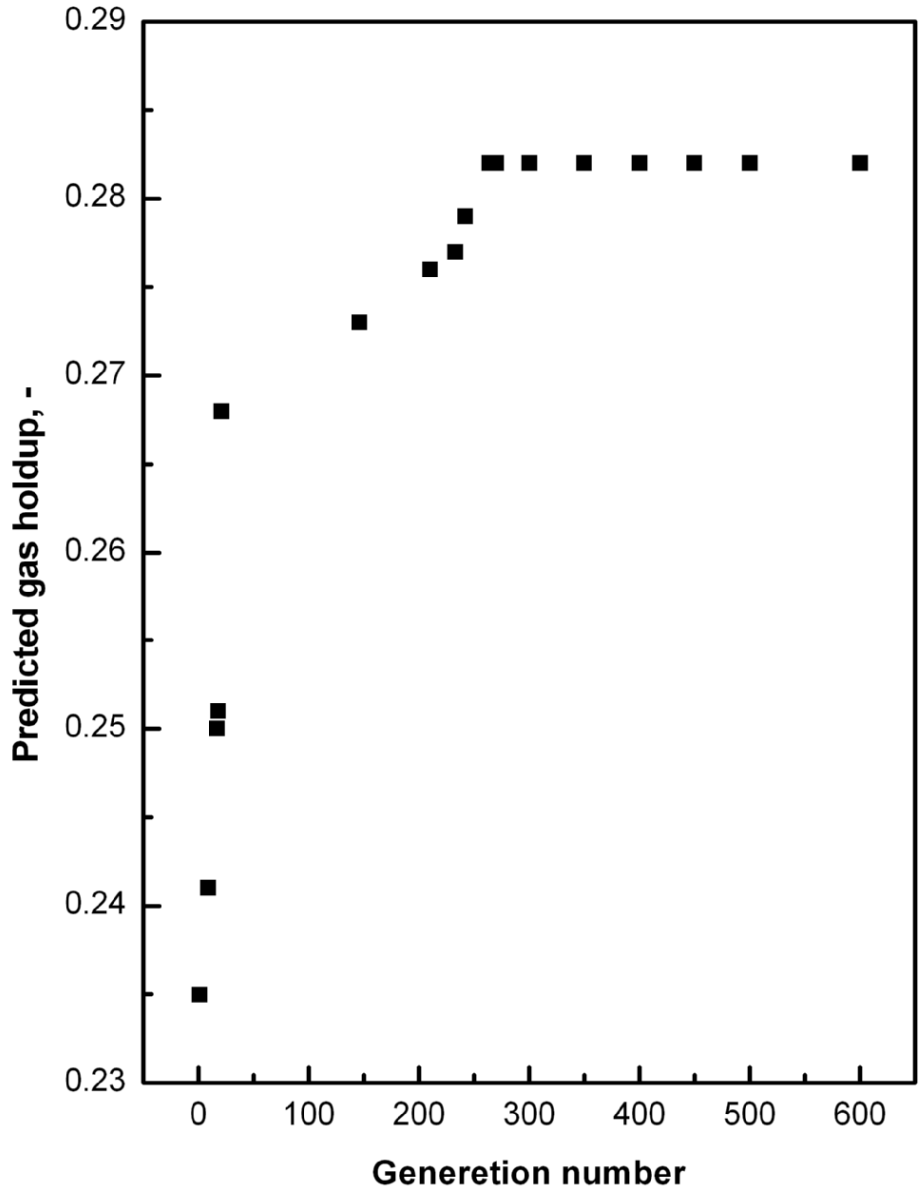

Fig. 12. Convergence curve.

Table 1
Scope of the experiment

A. Experimental conditions

Parameter	**Range**
Superficial gas velocity	$0.0212 < U_g < 0.1274$ m/s
Superficial liquid velocity	$0.0212 < U_l < 0.1486$ m/s
Initial static bed height	17.1, 21.3, 25.6 and 30.1 cm

B. Properties of gas, liquid and solid phase

Gas phase	**Density (kg/m^3)**	**Viscosity (Pa.s)**	**Surface tension (kg/m^2)**
Air at 30^0C	1.166	1.794×10^{-5}	-
Liquid phase (at 30^0C)			
Water	995.7	0.000798	0.0712
6% glycerol solution	1009.7	0.000984	0.0706
12% glycerol solution	1024.0	0.001082	0.0701
18% glycerol solution	1039.0	0.001268	0.0696
24% glycerol solution	1054.0	0.001567	0.0691
30% glycerol solution	1068.6	0.001852	0.0685

Solid phase	**Particle Size, mm**	**Particle density (kg/m^3)**
Glass beads	1.55	2253
	2.18	2216
	3.07	2253
	4.05	2270
	6.29	2470

Table 2
Wald Confidence Interval

Parameter	Estimate	A.S.E.	Param/ASE	Lower < 95%> Upper
Mo	0.050	0.003	14.795	0.043 0.057
Eo	0.203	0.008	18.637	0.140 0.174
Fr_L	-0.093	0.002	-47.202	-0.097 -0.089
Fr_g	0.401	0.001	267.223	0.398 0.404
β_d	-0.096	0.115	-0.834	-0.323 0.131
d_r	0.081	0.008	9.836	0.065 0.097
h_r	0.026	0.016	1.655	-0.005 0.058